Statistical mechanical description of the parking-lot model for vibrated granular materials

G. Tarjus and P. Viot

Laboratoire de Physique Théorique des Liquides, Université Pierre et Marie Curie, 4 place Jussieu, 75252 Paris Cedex 05, France
(Received 7 July 2003; published 30 January 2004)

We apply the statistical mechanical approach proposed by Edwards and co-workers to the parking-lot model, a model that reproduces the main features of the phenomenology of vibrated granular materials. We first build the compactivity-based measure for the case of vanishingly small tapping strength and then generalize the approach to finite tapping strengths by introducing a "thermodynamic" parameter, the available volume for particle insertion, in addition to the particle density. This description is able to take into account the various memory effects observed in vibrated granular media. Although not exact, the approach gives a good description of the behavior of the parking-lot model in the regime of slow compaction.

I. INTRODUCTION

Granular media are athermal, out-of-equilibrium systems which would be useful to describe within a statistical mechanical framework. A given macrostate of such a system characterized by a fixed density of grains (consider for simplicity a packing of monodisperse spherical particles) is very likely to be associated with an exponentially large number of microstates or particle configurations. How the packing was prepared (by pouring, shaking, shearing, etc.) may influence its properties and change the way the associated particle configurations are sampled when repeating over the same experimental protocol. However, the simplest hypothesis, put forward by Edwards and his co-workers [1–4], is that all microstates characterized by a given average density are equiprobable. With this "flat" (microcanonical) measure, one can build a statistical mechanical framework in which entropy, i.e., the logarithm of the number of microstates, is the relevant thermodynamic potential. This approach has recently been the focus of an intense research activity, in connection with a series of experiments performed on weakly vibrated granular materials [5–9] and with a theoretical description of out-of-equilibrium glassy systems based on the concept of effective temperature [10–14].

In the past few years, the hypothesis of Edwards and co-workers has been tested on many models, virtually all of them being lattice models with some kind of "tapping" kinetics [15–33]. In the absence of experimental tests of this approach (see, however, Ref. [6]), such theoretical studies are expected to better circumscribe the conditions of validity of the statistical mechanical description. (Presumably, only "approximate validity" can be expected since, aside from specific mean-field models [10,14], such a simplified description of out-of equilibrium situations in terms of a small number of "thermodynamic" parameters is unlikely to be exact.)

In this paper, we consider a statistical mechanical approach for the one-dimensional model of random adsorption-desorption of hard particles [34–36], also known as the parking-lot model [6]. This latter is a microscopic, off-lattice model that mimics many features of the compaction of a vibrated column of grains. Besides a qualitative description of the phenomenology of weakly tapped granular media

[6,7,37–41], the interest of the model is that exact analytical results can be derived or, when not possible, very accurate numerical data can be obtained from computer simulations. In the following section, we briefly introduce the parking-lot model and we discuss its connection to vibrated granular materials. In Sec. III, we consider the limit of vanishingly small (but nonzero) tapping intensity; we construct for this case a description based on a microcanonical (flat) measure in which all "blocked" states are considered as equiprobable and we compare the resulting predictions to the exact behavior. In the following section, we generalize the study to the case of a finite tapping intensity: we consider what appears to be the simplest, yet compatible with known experimental observations, generalization of the Edwards' formalism. Finally, we discuss the merits and limitations of the approach.

II. THE MODEL AND ITS CONNECTION TO VIBRATED GRANULAR MATERIALS

The parking-lot model is a one-dimensional random adsorption-desorption process of hard rods on a line. Hard rods of length σ are deposited at random positions on a line at rate k_+ and are effectively inserted if they do not overlap with predeposited rods; otherwise they are rejected. In addition, all deposited particles can desorb, i.e., be ejected from the line at random with a rate k_-. Time is measured in units of $1/k_+$, length in units of σ, and the model depends on one control parameter $K = k_+/k_-$. When no desorption is present ($k_- = 0$), the model reduces to the purely irreversible one-dimensional random sequential adsorption (RSA) process [42–44], and all the properties of the system as a function of time are known exactly [44–46]. In addition, for $1/K$ nonstrictly equal to zero, the competition of mechanisms between adsorption and desorption allows the system to reach a steady state that is nothing but an equilibrium fluid of hard rods at constant activity $1/K$: there too, all properties are known exactly.

The densification kinetics of the parking-lot model at constant K is described by

$$\left. \frac{\partial \rho}{\partial t} \right|_K = \Phi(t) - \frac{\rho}{K}, \qquad (1)$$

where $\rho(t)$ is the density of hard rods on the line at time t (recall that $\sigma \equiv 1$) and $\Phi(t)$ is the fraction of the line that is available at time t for inserting a new particle, i.e., the probability associated with finding an interval free of particles (a "gap") of length at least 1. The quantities ρ and Φ can be calculated from the one-gap distribution function $G(h,t)$ which is the density of gaps of length h at time t via a number of "sum rules":

$$\rho(t) = \int_0^\infty dh\, G(h,t), \qquad (2)$$

$$1 - \rho(t) = \int_0^\infty dh\, hG(h,t), \qquad (3)$$

$$\Phi(t) = \int_1^\infty dh\, (h-1)G(h,t). \qquad (4)$$

The evolution with time of the one-gap distribution function can itself be described by a kinetic equation that involves two-gap distribution functions, and so on [37]. Except for the two above mentioned limits (RSA when $k_- = 0$, equilibrium when $t \to +\infty$), the infinite hierarchy of coupled equations cannot be solved analytically and one must resort to approximate treatments and computer simulations, as described in previous papers [37–40].

First introduced in the context of protein adsorption at liquid-solid interfaces [34–36], the random adsorption-desorption model has recently been applied to the description of weakly vibrated granular materials [6,7,37–41]. The connection between the parking-lot model and these latter is made by regarding the particles on the line as an average layer of grains in the vibrated column. Time measures the number of taps whose effect is to eject particles from the layer; ejection is followed by the arrival at random of particles in the layer, which mimics the gravity-driven relaxation step in the experiment. Considering that the main influence of the intensity of the tapping is to determine the average number of particles ejected at each tap (this number being an increasing function of intensity) leads to associate $1/K$ with the tapping strength. A two-dimensional version of the model with some polydispersity of the particles would clearly be more realistic, but one does not expect this to change the qualitative features of the model [43]. A more serious caveat is the absence of an explicit account of the mechanical stability of the particle packings: stability is only implicitly described by the fact that the particles are blocked on the line between two successive desorption events.

Despite drastic simplification of the situation encountered in vibrated granular materials, the parking-lot model reproduces at a qualitative level most of the relevant phenomenology: (i) for large rate K corresponding to weak tapping intensity, compaction proceeds very slowly and can be effectively described by an inverse logarithm of time [34,35,38,37]; (ii) stronger tapping leads to faster initial compaction but to less effective asymptotic packing [37]; (iii) the slow densification kinetics leads to irreversibility effects and to the observation of two curves for the packing

density as a function of tapping intensity [37], one essentially reversible and another irreversible depending on the experimental protocol chosen [39]; (iv) the power spectrum of the density fluctuations near the steady state is distinctly nonLorenztian and displays a power-law regime at intermediate frequencies [6,7,39–41]; (v) nontrivial memory effects are observed when changing abruptly the tapping intensity [39,40].

Note that, as recently studied for a one-dimensional model with tapping dynamics [30], the parking-lot model could also be used, via the introduction of two kinds of particles, to describe the segregation phenomena with the so-called Brazil nut [47,48] and reverse Brazil nut [49,50] effects.

III. LIMIT OF VANISHINGLY SMALL TAPPING INTENSITY: $K \to \infty$

In this limit, ejection of one particle from the line is followed by an infinite number of insertion trials until one or, seldom, two new particles are added. The stable or "blocked" configurations are thus those for which no more particle insertions are possible (recall that once successfully inserted particles cannot move on the line), i.e., all configurations of nonoverlapping rods such that the available line fraction Φ is zero, or, equivalently, such that all gaps between neighboring particles are smaller than a particle size (here taken as unity). The prescription proposed by Edwards and co-workers for constructing a statistical mechanical description of this system is then to consider that all such "blocked" configurations at a fixed density ρ are equiprobable (flat or microcanonical distribution).

Consider a line of length L with N particles. With periodic boundary conditions, this system has also N gaps between neighboring particles. Denoting by $h_1, h_2, \ldots, h_N$ the lengths of these gaps, the total number of "blocked" configurations is given by the configurational integral calculated under the constraint that $h_i < 1$ for $i = 1, \ldots, N$, namely,

$$Z(L,N) = \int_0^1 \cdots \int_0^1 \left(\prod_{i=1}^N dh_i \right) \delta\left(L - N - \sum_{i=1}^N h_i \right), \quad (5)$$

which by using the integral representation of the δ-function can be rewritten as

$$Z(L,N) = \int_C dz\, e^{z(L-N)} \left(\prod_{i=1}^N \int_0^1 dh_i\, e^{-zh_i} \right), \qquad (6)$$

where C denotes a closed contour. Integrating over the h_i's yields

$$Z(L,N) = \int_C dz \exp\left\{ L\left[z(1-\rho) + \rho\ln\left(\frac{1-\exp(-z)}{z} \right) \right] \right\}, \qquad (7)$$

where $\rho = N/L$. In the macroscopic limit where $N \to \infty$, $L \to \infty$, with a fixed ρ, the above expression can be evaluated through a saddle-point method, which gives

$$Z(L,N) \simeq \exp[Ls(\rho)], \qquad (8)$$

where $s(\rho)$, the entropy density, is expressed as

$$s(\rho) = (1-\rho)z + \rho \ln\left(\frac{1-e^{-z}}{z}\right), \qquad (9)$$

where $z \equiv z(\rho)$ is the solution of the saddle-point equation

$$\left(\frac{1-\rho}{\rho}\right) = \frac{1}{z} - \frac{e^{-z}}{1-e^{-z}}. \qquad (10)$$

In Edwards' language, $1/z = (\partial(Ls)/\partial L|_N)^{-1}$ is the compactivity (up to a trivial constant) [51]. In an equilibrium system of hard rods, i.e., without the constraint that all gaps have a length smaller than 1, $z(\rho)$ would simply be equal to $P/(k_BT) = \rho/(1-\rho)$ where P is the pressure.

By Legendre transforming the entropy $S(L,N) = Ls$, one obtains a new potential

$$Y(N,z) = -S(L,N) + zL = N\left[z - \ln\left(\frac{1-e^{-z}}{z}\right)\right] \qquad (11)$$

such that $\partial(Y)/\partial z|_N = \langle L \rangle$ and from which one can obtain the fluctuations of the system size,

$$\langle L^2 \rangle - \langle L \rangle^2 = -\left.\frac{\partial^2(Y)}{\partial z^2}\right|_N = -N\left.\frac{\partial(1/\rho)}{\partial z}\right|_N. \qquad (12)$$

By combining the above expression with Eq. (10), one derives the fluctuations of the density,

$$L(\langle \rho^2 \rangle - \langle \rho \rangle^2) = \frac{\rho^3}{N}(\langle L^2 \rangle - \langle L \rangle^2) = \rho^3\left(\frac{1}{z^2} - \frac{e^{-z}}{(1-e^{-z})^2}\right). \qquad (13)$$

In the constrained microcanonical ensemble, one can also calculate the gap distribution functions. The one-gap distribution function $G(h;\rho)$, which gives the density of gaps of length h, is obtained from

$$G_{Ed}(h;\rho) = \frac{1}{LZ(L,N)} \sum_{i=1}^{N} \int_0^1 \cdots \int_0^1 \left(\prod_{j=1,j\neq i}^{N} dh_j\right)$$

$$\times \delta\left(L - N - h - \sum_{j=1,j\neq i}^{N} h_j\right). \qquad (14)$$

By using the same method as before one finds that

$$G_{Ed}(h;\rho) = \begin{cases} \rho\dfrac{z}{1-e^{-z}}e^{-zh} & \text{for } h<1 \\ \\ 0 & \text{for } h>1, \end{cases} \qquad (15)$$

where z is the solution of Eq. (10). It is easy to check that the above expression satisfies the two sum rules, Eqs. (2) and (3).

The higher-order gap distribution functions are obtained along the same lines, and they satisfy a factorization property analogous to that found for an equilibrium system of hard rods, i.e.,

$$G_{Ed}(h,h';\rho) = G_{Ed}(h;\rho)G_{Ed}(h';\rho), \qquad (16)$$

$$G_{Ed}(h,h',h'';\rho) = G_{Ed}(h;\rho)G_{Ed}(h';\rho)G_{Ed}(h'';\rho), \qquad (17)$$

etc.

The one-gap distribution function $G_{Ed}(h;\rho)$ is directly related to the nearest-neighbor pair distribution function that represents the probability of finding two neighboring particles whose centers are separated by a distance $1+h$. It is also possible to calculate the full pair distribution function $g_{Eq}(r;\rho)$ via a method which closely follows that which was developed for the equilibrium system of hard rods [52]. The steps of the calculation are detailed in Appendix A, and the final result reads

$$g_{Ed}(r;\rho) = \frac{1}{\rho} \sum_{m=1}^{\infty} \frac{(r-m)^{m-1}}{(m-1)!}\left(\sum_{k=0}^{m} C_m^k(-1)^k \theta(r-m-k)\right)$$

$$\times \left(\frac{z}{1-e^{-z}}\right)^m e^{-z(r-m)}, \qquad (18)$$

where $\theta(x)$ is the Heaviside step function and z is the solution of Eq. (10). For comparison, we give the equilibrium pair distribution function [52]

$$g_{eq}(r;\rho) = \frac{1}{\rho} \sum_{m=1}^{\infty} \theta(r-m)\frac{(r-m)^{m-1}}{(m-1)!}\left(\frac{\rho}{1-\rho}\right)^m$$

$$\times e^{-[\rho/(1-\rho)](r-m)}. \qquad (19)$$

We can now compare the above results derived under the condition of equiprobability of the "blocked" configurations with the exact ones obtained either analytically or numerically. When $K \to \infty$, analytical results are available in the two limits, $t = 0^+$, which corresponds to the purely irreversible RSA process at the jamming limit where no more particles can be inserted [44], and $t \to +\infty$, which corresponds to a close-packed state with $\rho = 1$.

For the RSA at the jamming limit, closed-form expressions have been derived for the saturation density [44],

$$\rho_{JL} = \int_0^{\infty} dt \exp\left(-2\int_0^t du \frac{1-e^{-u}}{u}\right) \simeq 0.747\,59 \ldots, \qquad (20)$$

for the density fluctuations [45], for the gap distribution functions [46], and for the pair distribution function [45]. (The expressions are given in Appendix B.) When comparing to the approximate results at the same density, ρ_{JL} one finds qualitative differences. Most notably, (i) the exact one-gap distribution function displays a logarithmic divergence at contact between particles ($h \to 0^+$),

$$G(h;\rho_{JL}) \simeq -e^{-2\gamma}\ln(h), \qquad (21)$$

where γ is the Euler constant, (ii) the exact multigap distribution functions do not reduce to products of the one-gap functions, (iii) the exact pair distribution function has a superexponential decay at large distances,

$$g(r,\rho_{JL})-1 \sim \frac{1}{\Gamma(r)}, \quad r \to \infty, \tag{22}$$

all features that are missed by the flat-measure expressions, since

$$G_{Ed}(h=0;\rho_{JL})=\rho_{JL}\frac{z(\rho_{JL})}{1-z(\rho_{JL})}, \tag{23}$$

$$g_{Ed}(r,\rho_{JL})-1 \sim -e^{z(\rho_{JL})r}, \quad r \to \infty, \tag{24}$$

and the multigap functions satisfy a factorization property, Eqs. (16) and (17).

Quantitatively, one can also see differences, e.g., in the density fluctuations, the exact result at jamming being $L(\langle\rho^2\rangle-\langle\rho\rangle^2) \simeq 0.038$ to be compared with $L(\langle\rho^2\rangle-\langle\rho\rangle^2)_{Ed} \simeq 0.028$.

Such observations, which generalize to an off-lattice model the results obtained by de Smedt *et al.* [31,32] for random and cooperative sequential adsorption models on a one-dimensional lattice, are in fact to be expected: it has been shown that the RSA process generates configurations of hard particles that are sampled from a probability distribution that is "biased" when compared to a uniform (flat) distribution [53,54].

As the system further evolves with time at vanishingly small tapping intensity, compaction takes place beyond the RSA saturation density, and the difference between the actual properties of the system and those predicted by the flat measure diminishes.

Figure 1 compares the variation with ρ (for $\rho \geq \rho_{JL}$) of the density fluctuations of the parking-lot model (simulation results) with the approximate result, Eq. (13), and the equilibrium curve, $L(\langle\rho^2\rangle-\langle\rho\rangle^2)_{eq}=\rho(1-\rho)^2$. The prediction is in fair agreement with the simulation data, especially for intermediate densities, but it reaches too rapidly the equilibrium curve that (slightly) overestimates the exact result. (Note that simulating the system becomes very time consuming as compaction goes on and, in practice, we cannot go beyond a density of about 0.93; the infinite-time limit should of course be $\rho=1$.) However the description improves upon the equilibrium curve and gives the proper shape of the density dependence with an inflection around $\rho \simeq 0.87$. The closeness of the flat-measure result and the equilibrium one (the former being with the constraint that no gaps have a length larger than 1) at high density is illustrated in Fig. 2 where we show the entropy density versus particle density.

In Figure 3 we have displayed on a logarithmic-linear plot the predicted and computed one-gap distribution functions for four different densities. The approximation is too small at small h for $\rho=0.75$, which is reminiscent of the missing the logarithm divergence at the RSA jamming limit $\rho_{JL}=0.747$ (see above). Otherwise the agreement with the simulation
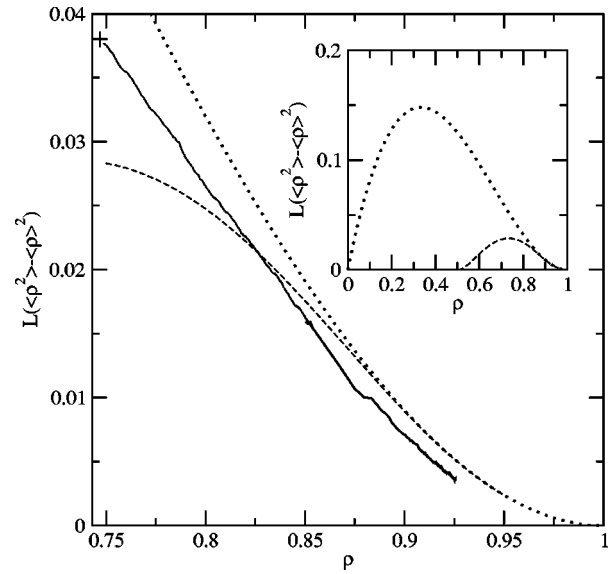

FIG. 1. Density fluctuations of the parking-lot model when $K \to +\infty$ for densities above the RSA jamming limit. Simulation data (obtained by averaging 20 000 different runs for a system size $L = 500$) are shown as the full line, the flat-measure approximation corresponds to the dashed curve, and the equilibrium result to the dotted curve. The inset displays the density fluctuations at equilibrium and in the approximation for a larger range of densities.

data is very good (recall that this is a log-linear plot). For $h>1$, the description is exact since $G_{Ed}(h>1)=0$.

Finally, we have plotted in Figs. 4–6 the pair distribution functions (simulation data, approximation, equilibrium curve) for three different densities: $\rho=0.77$, $\rho=0.82$, and $\rho=0.92$. The flat measure is an improvement upon the equi-
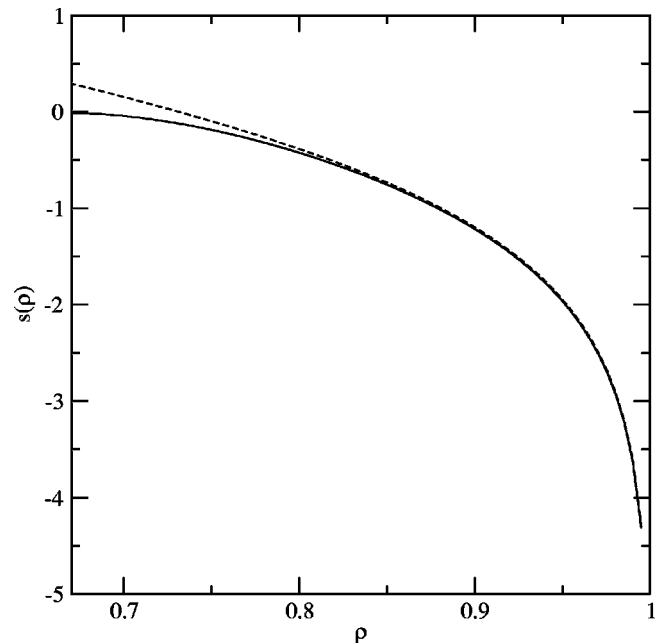

FIG. 2. Entropy density vs particle density for a hard-rod system: Edwards entropy for the parking-lot model when $K \to \infty$ (full curve) and equilibrium entropy (dashed curve).
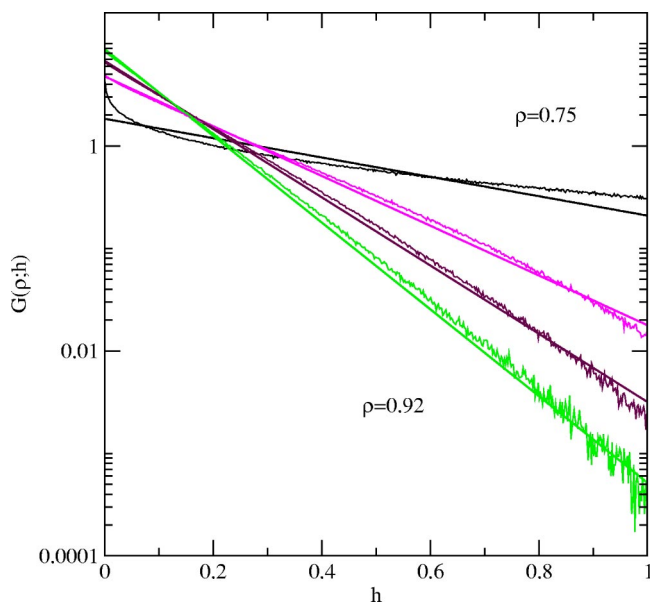
FIG. 3. Parking-lot model when $K \to +\infty$: log-linear plot of the one-gap distribution function vs h for several densities: from top to bottom $\rho = 0.75, 0.85, 0.89, 0.92$. Comparison of simulation data (wavy line) and flat-measure approximation (full curve).

librium curve, but even at $\rho = 0.82$ (Fig. 5), it somewhat overestimates the oscillations at large distances. For $\rho = 0.92$ (Fig. 6), the difference between the three curves is barely visible. Note that for $1 \leq r < 2$, the pair distribution function is equal to the nearest-neighbor distribution function, hence to the one-gap distribution function shown in Fig. 3
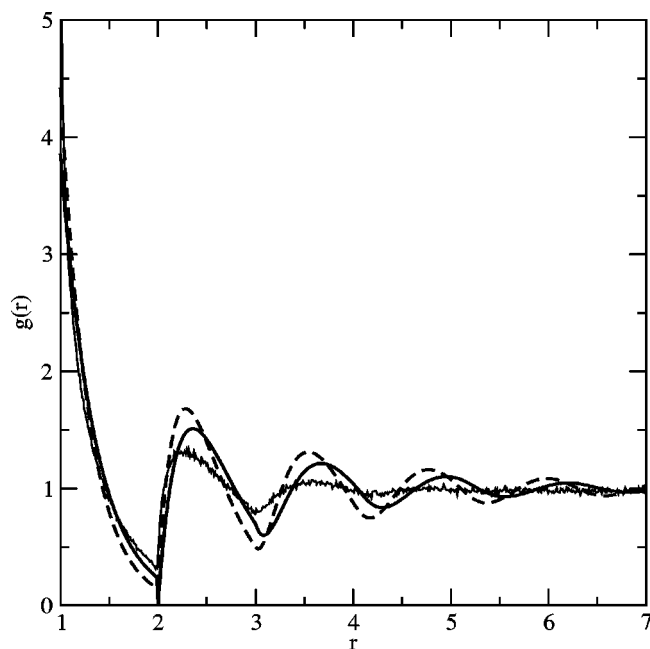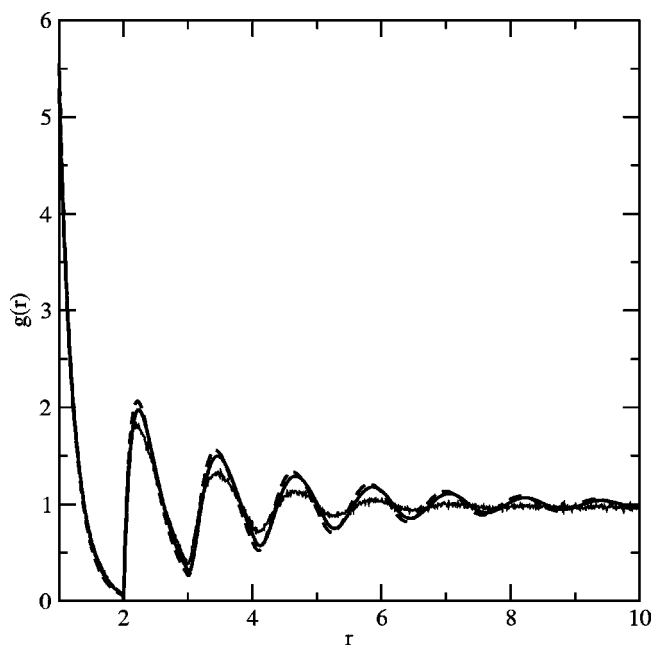

FIG. 5. Same as Fig. 4 for $\rho = 0.82$.

IV. FINITE TAPPING INTENSITY: K FINITE

When the tapping intensity, i.e., $1/K$, is finite, one must modify the definition of the stable or "blocked" states. Indeed, for finite K, the configuration of hard rods obtained after a desorption-adsorption event is no longer characterized by $\Phi = 0$, and the gaps between particles can be larger than one. One also knows that the tapping intensity $1/K$ is not the proper "thermodynamic" parameter to add to the density in order to characterize the macrostate of the system in a statistical mechanical approach: the memory effect observed experimentally [8] and reproduced by the present parking-lot
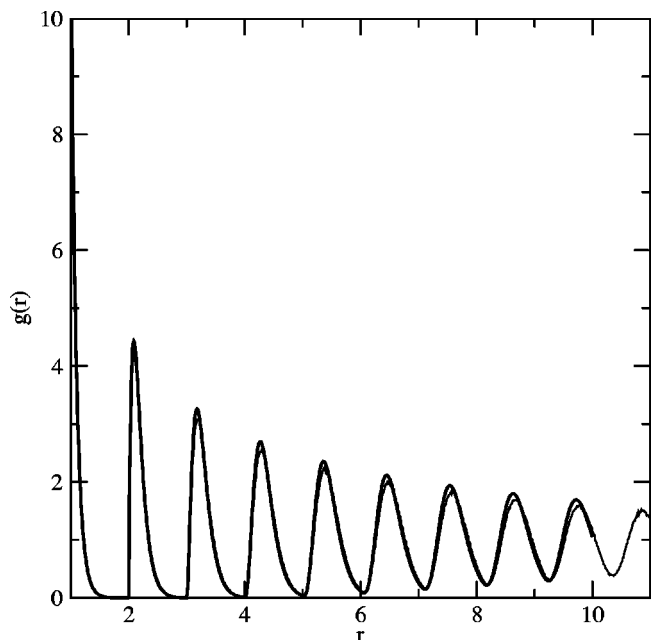

FIG. 4. Pair distribution function in the parking-lot model when $K \to +\infty$ at $\rho = 0.77$: simulation data (wavy curve), flat-measure approximation (full curve), and equilibrium (dashed curve).
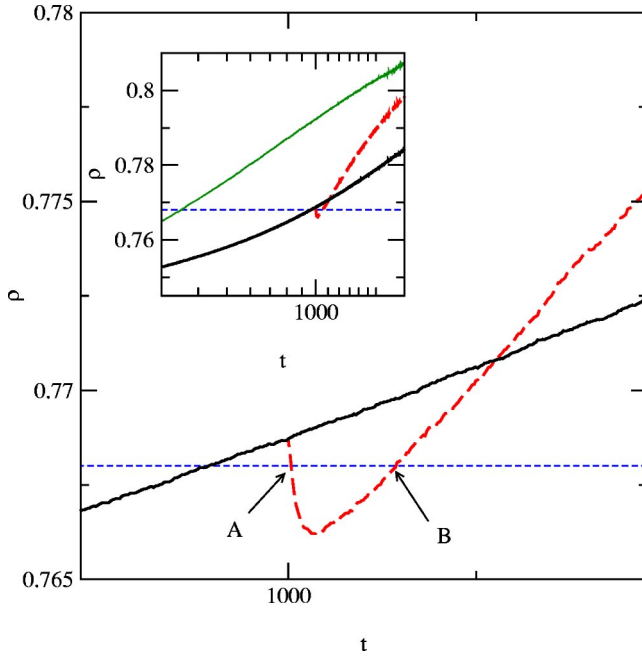

FIG. 6. Same as Fig. 4 for $\rho = 0.92$.

FIG. 7. Memory effect in the parking-lot model. The full curve corresponds to a process at constant $K=2000$ whereas the dashed curve shows the kinetics when K is switched from 2000 to 500 at $t_s=1000$. The points A and B correspond to states with equal density, equal value of $K=500$, but different further evolution. The inset shows the phenomenon with a larger scale (upper curve, constant $K=500$; lower curve, constant $K=2000$).

model (see above) implies that the system can be found in states, characterized by the same density ρ and the same tapping intensity $1/K$, that however evolve differently under further tapping with the same intensity $1/K$; as illustrated in Fig. 7, the density may increase in one case and decrease in another.

If the tapping intensity is not an appropriate thermodynamic parameter, a natural choice for a two-parameter statistical mechanical description appears to be Φ, the available line fraction, that one can use in conjunction with the density ρ. A nonzero Φ generalizes to a finite tapping intensity, the prescription uses for vanishingly small intensity, namely, $\Phi=0$, and Φ is also directly relevant for describing the compaction kinetics, as shown by Eq. (1). We thus consider a statistical mechanical ensemble in which all configurations of nonoverlapping hard rods characterized by fixed values of ρ and Φ are equally probable.

Denoting by A the total length available for insertion for a particle center ($A=\Phi L$), the configurational integral with the constraints of fixed A, fixed system size L, and fixed number of particles N is given by

$$Z(L,N,A)=\int_0^L \cdots \int_0^L \prod_{i=1}^N dh_i \delta\left(L-N-\sum_{i=1}^N h_i\right)$$
$$\times \delta\left(A-\sum_{i=1}^N \theta(h_i-1)(h_i-1)\right), \qquad (25)$$

which can be rewritten as before as

$$Z(L,N,A)=\int_C dz \int_{C'} dy \exp\left\{L\left[z(1-\rho)+y\Phi\right.\right.$$
$$\left.\left.+\rho\ln\left(\frac{z+y[1-\exp(-z)]}{z(z+y)}\right)\right]\right\}, \qquad (26)$$

where C and C' denote two closed contours. In the macroscopic limit, $N\to\infty$, $L\to\infty$, $A\to\infty$ with ρ and Φ fixed, one can again use a saddle-point method to evaluate the integrals, which leads to

$$Z(L,N,A)\simeq\exp[Ls(\rho,\Phi)], \qquad (27)$$

where $s(\rho,\Phi)$ is expressed as

$$s(\rho,\Phi)=(1-\rho)z+y\Phi+\rho\ln\left(\frac{z+y[1-\exp(-z)]}{z(z+y)}\right), \qquad (28)$$

with $z\equiv z(\rho,\Phi)$ and $y\equiv y(\rho,\Phi)$ solutions of the two coupled equations

$$\left(\frac{1-\rho}{\rho}\right)=\frac{1}{z}+\frac{1}{z+y}-\frac{1+ye^{-z}}{z+y(1-e^{-z})}, \qquad (29)$$

$$\frac{\Phi}{\rho}=\frac{1}{z+y}-\frac{1-e^{-z}}{z+y(1-e^{-z})}. \qquad (30)$$

$z=(\partial S/\partial L)_{N,A}$ can again be considered as the inverse of the "compactivity," but an additional intensive parameter $y=(\partial S/\partial A)_{N,L}$ is needed.

A double Legendre transformed potential $Y(N,z,y)$ can be introduced as

$$Y(N,z,y)=-Ls(\rho,\Phi)+zL+yA$$
$$=N\left[z-\ln\left(\frac{z+y[1-\exp(-z)]}{z(z+y)}\right)\right]. \qquad (31)$$

Then, $\partial(Y)/\partial z|_{N,y}=\langle L\rangle$ and $\partial(Y)/\partial y|_{N,z}=\langle A\rangle$, and the fluctuations in L and A are given by

$$\langle L^2\rangle-\langle L\rangle^2=-\left.\frac{\partial^2(Y)}{\partial z^2}\right|_{N,y}=-N\left.\frac{\partial(1/\rho)}{\partial z}\right|_y, \qquad (32)$$

$$\langle A^2\rangle-\langle A\rangle^2=-\left.\frac{\partial^2(Y)}{\partial y^2}\right|_{N,z}=-N\left.\frac{\partial(\Phi/\rho)}{\partial y}\right|_z, \qquad (33)$$

$$\langle LA\rangle-\langle L\rangle\langle A\rangle=-\left.\frac{\partial^2(Y)}{\partial z\partial y}\right|_N$$
$$=-N\left.\frac{\partial(\Phi/\rho)}{\partial z}\right|_y$$
$$=-N\left.\frac{\partial(1/\rho)}{\partial y}\right|_z. \qquad (34)$$

By using the saddle-point equations, Eqs. (29) and (30), one arrives at the following expression for the fluctuations of ρ:

$$L(\langle\rho^2\rangle-\langle\rho\rangle^2)=\frac{\rho^3}{N}(\langle L^2\rangle-\langle L\rangle^2)$$

$$=\rho^3\left(\frac{1}{z^2}+\frac{1}{(z+y)^2}-\frac{1+(2+z+y)ye^{-z}}{[z+y(1-e^{-z})]^2}\right).$$

$$(35)$$

Similar expressions are obtained for the fluctuations of Φ and the cross fluctuations of ρ and Φ, but are not shown here.

The gap distribution functions can also derived by following the same method as in the preceding section. This leads to

$$G_{Ed}(h;\rho)=\begin{cases}\rho\dfrac{z(z+y)}{z+y(1-e^{-z})}e^{-zh} & \text{for } h<1\\[4mm]\rho\dfrac{z(z+y)}{z+y(1-e^{-z})}e^{-[zh+y(h-1)]} & \text{for } h>1,\end{cases}$$

$$(36)$$

whereas the multigap distribution functions satisfy the factorization property, e.g., $G_{Ed}(h,h';\rho,\Phi)=G_{Ed}(h;\rho,\Phi)G_{Ed}(h';\rho,\Phi)$. Notice that the one-gap distribution function is a piecewise continuous function that obeys the exact sum rules, Eqs. (2)–(4). It is also worth pointing out that the results of Sec. III ($K\to\infty$) can be recovered by taking the limit $y\to\infty$ in the above equations. Finally, the pair distribution function can be derived along the same lines as shown before and in Appendix A, but the calculation is too tedious and not sufficiently insightful to be presented here.

A comparison between the two-parameter flat measure and the simulation data is shown in Figs. 8 and 9 for the density fluctuations with $K=500$ and $K=5000$, respectively. We have also plotted the equilibrium curve, $L(\langle\rho^2\rangle_{eq}-\langle\rho\rangle^2_{eq})=\rho(1-\rho)^2$, and the one-dimensional RSA curve [45] up to ρ_{JL}. The predictions are good but not perfect. They display the proper nontrivial shape of the ρ dependence, in contradistinction to the equilibrium curve, but there is a significant underestimation of the fluctuations in the density range around the RSA jamming limit. Note that at high density the approximation is in very good agreement with the simulation data (at least for $K=500$) and does not merge too rapidly with the equilibrium curve as seen above for the case $K\to\infty$.

The one-gap distribution functions shown on a log-linear plot in Fig. 10 illustrate also the overall good agreement between the two-parameter measure predictions and the simulation data. The approximation captures the change of the slope of the one-gap distribution function that occurs for $h>1$; but the curvature seen in the simulation data for h slightly larger than 1 is not correctly reproduced by the two-parameter measure which predicts an exponential decay with
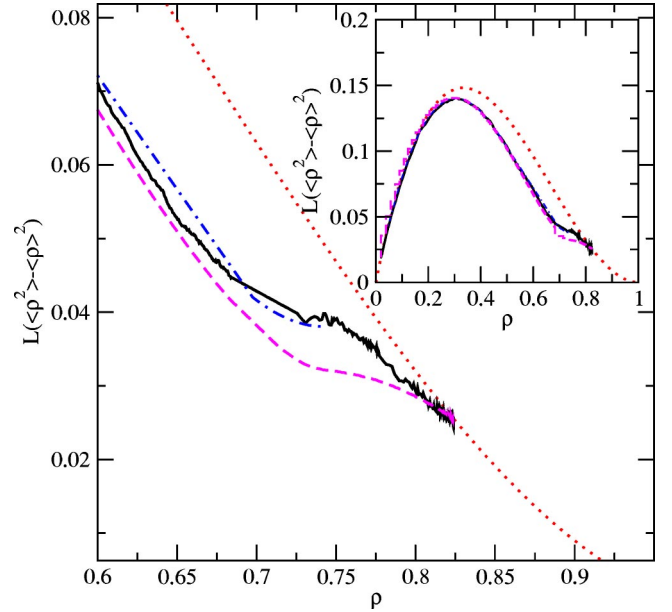

FIG. 8. Density fluctuations as a function of ρ for $K=500$. The dotted curve corresponds to the equilibrium density fluctuations, the dot-dashed curve to the RSA result, the dashed curve to the two-parameter approximation, and the wavy line to the simulation data (obtained by averaging 15 000 different runs for a system size $L=400$). The inset displays the same curves for a larger range of densities.

a factor equal to $z+y$ [see Eq. (36)]. Again, this discrepancy is larger for densities around of the RSA jamming limit (the two intermediate sets of curves in Fig. 10).

V. CONCLUSION

In this work we have applied the statistical mechanical approach based on the microcanonical ("flat") measure pro-
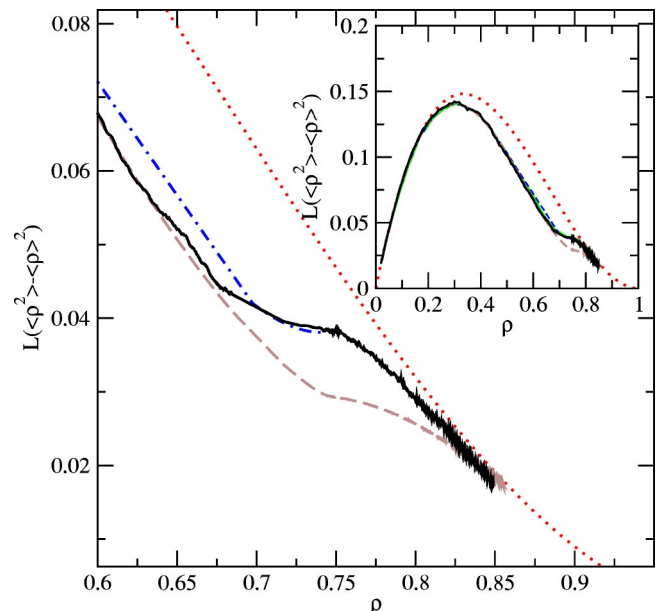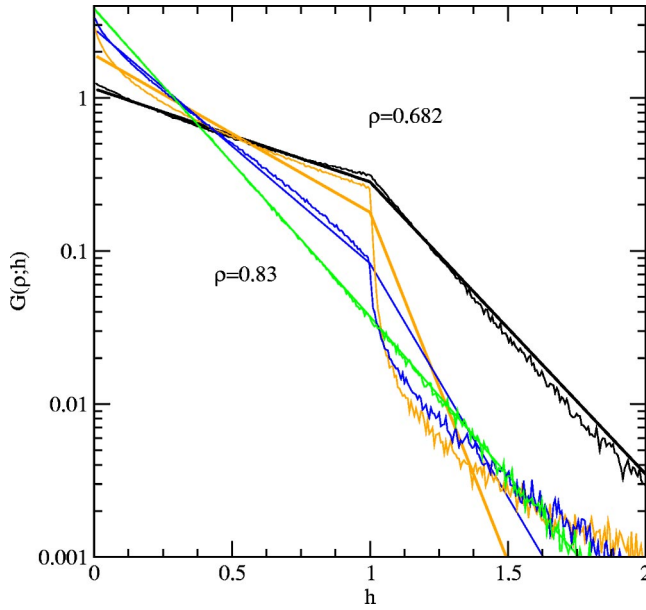

FIG. 9. Same as Fig. 8 for $K=5000$.

FIG. 10. Parking-lot model when $K=500$: log-linear plot of the one-gap distribution function vs h for several densities: from top to bottom in the middle of the figure $\rho=0.682, 0,748, 0.790, 0.83$. Comparison of simulation data (wavy line) and two-parameter approximation (full curve). For $\rho=0.83$, there is virtually no difference between the two curves.

posed by Edwards and co-workers to the out-of-equilibrium situation obtained in the parking-lot model. This latter is a microscopic off-lattice model that reproduces the major features of the phenomenology of vibrated granular materials. In the statistical mechanical description, a macrostate of the system is characterized by fixed values of two macroscopic quantities, the particle density ρ and the available line fraction Φ (or rather fixed values of three extensive parameters: the number of particles, the system size, and the total length available for insertion of particles), and all configurations of nonoverlapping particles with fixed ρ and Φ are taken as equiprobable.

We show that such an approach misses some of the qualitative signatures of the limiting case of a purely irreversible adsorption process (RSA) at the jamming limit. However, at higher densities, i.e., in the slow (logarithmic) compaction regime, it gives a good, yet not perfect, quantitative description of many observable quantities (fluctuation, distribution functions). The choice of Φ as an additional "thermodynamic" parameter is able to account for situations, encountered in various memory effects, in which macrostates characterized by the same density and the same tapping intensity can nonetheless be different.

The fact that a "thermodynamic" approach gives a good description of a model of vibrated granular media is promising. In the one-dimensional model studied here, the generalized "equation of state" associated with the compactivity-based microcanonical distribution can be analytically derived so that one can make theoretical predictions concerning, e.g., the density fluctuations or the structure of the configurations. However, one still faces the task of predicting the state of the system for a given preparation, i.e., for a given time (number

of taps) and a given protocol for the tapping intensity. We are presently working on this problem.

APPENDIX A: PAIR DISTRIBUTION FUNCTION IN THE CONSTRAINED MICROCANONICAL ENSEMBLE ($K \to \infty$) AND AT EQUILIBRIUM

We introduce the probability density $\Psi_m(\xi)$ of finding two given particles at a relative distance ξ, such that there is exactly $m-1$ particles between them; this function can be expressed in terms of the partition function as

$$\Psi_m(\xi) = \frac{Z(\xi, m-1)Z(L-\xi, N-m)}{Z(L,N)}, \quad \text{(A1)}$$

where $Z(L,N)$ can be calculated either with the constrained microcanonical distribution or at equilibrium.

For large N, one can use the asymptotic expression of the partition function $Z(L,N) = e^{z(L-N)}\phi(z)^N$. At equilibrium $\phi(z) = 1/z$ whereas with the constrained microcanonical measure, one gets $\phi(z) = (1-e^{(-z)})/z$ and z given by Eq. (10). Therefore, the probability density is equal to

$$\Psi_m(\xi) = Z(\xi, m-1)\frac{1}{\phi(z)^m}e^{-z(\xi-m)} \quad \text{(A2)}$$

and, formally, the pair distribution function can be expressed as

$$g(r,\rho) = \frac{1}{\rho}\sum_{m=1}^{\infty}\Psi_m(r). \quad \text{(A3)}$$

For hard rods, the partition function $Z(\xi, m-1)$ is different from 0 for $\xi > m$. At equilibrium, one has for $\xi > m$

$$Z(\xi, m-1) = \frac{(\xi-m)^{m-1}}{(m-1)!} \quad \text{(A4)}$$

and $z = \rho/(1-\rho)$, which gives for the pair distribution function [52]

$$g_{eq}(r,\rho) = \frac{1}{\rho}\sum_{m=1}^{\infty}\frac{\theta(r-m)(r-m)^{m-1}}{(m-1)!(1/\rho-1)^m}\exp\left(-\frac{r-m}{1/\rho-1}\right) \quad \text{(A5)}$$

when $r > 1$, where $\theta(x)$ is the Heaviside function.

In the constrained microcanonical ensemble, the expression for $Z(\xi, m-1)$, hence for $\psi_m(r)$, involves $m+1$ contributions. For instance, $\Psi_1(r)$ is given by

$$\Psi_1(r) = [\theta(r-1) - \theta(r-2)]\frac{z}{1-e^{-z}}e^{-z(r-1)}. \quad \text{(A6)}$$

More generally

$$\psi_m(r) = \sum_{k=0}^{m}C_m^k(-1)^k\theta(r-m-k)\left(\frac{z}{1-e^{-z}}\right)^m e^{-z(r-m)}. \quad \text{(A7)}$$

Inserting Eq. (A7) into Eq. (A3) yields Eq. (18).

APPENDIX B: RSA EXPRESSIONS AT THE JAMMING LIMIT

For the one-dimensional RSA process, the one-gap distribution function at the jamming limit ($t \to \infty$) is given by [42,43]

$$G(h;\rho_{JL}) = \begin{cases} 2\int_0^\infty dt\, t k(t)^2 e^{(-th)} & \text{for } h<1 \\ 0 & \text{for } h>1, \end{cases} \quad (B1)$$

with

$$k(t) = \exp\left(-\int_0^t \frac{1-e^{-u}}{u} du\right). \quad (B2)$$

The pair distribution function can be expressed in a closed form by using the Laplace transform $\tilde{g}(s,t) = \int_0^{+\infty} dl\, e^{-sl} g(l+1,t)$. At the jamming limit, one has [45]

$$\tilde{g}(s,\rho_{JL}) = \frac{1}{\rho_{JL}^2}\left(\frac{1}{s}\left[\int_0^\infty dt_1 \frac{k(t_1)k(t_1+s)}{k(s)}\right]^2 \right.$$

$$-2\int_0^\infty dt_1 \frac{k(t_1)k(t_1+s)}{k(s)}\int_0^{t_1} dt_2 \frac{k(t_2)k(t_2+s)}{k(s)}$$

$$\left. \times \int_0^{t_2} dt_3 \frac{e^{-t_3}k^2(s)}{k^2(t_3+s)} B(s,t_3)\right). \quad (B3)$$

with

$$B(s,t) = \frac{1}{s+t} - \frac{1-e^{-(s+t)}}{(s+t)^2}. \quad (B4)$$

The expression for the density fluctuations follows from the above equation by taking the limit $s \to 0$ of the expression $\rho(1+2\rho[\tilde{g}(s,\rho_{JL})e^{-s}-1/s])$ [45]. This gives

$$L(\langle\rho^2\rangle-\langle\rho\rangle^2) = \rho_{JL}\left[-1+2\rho_{JL}-\frac{4}{\rho}\int_0^\infty dt_1 k^2(t_1)\right.$$

$$\times \int_0^{t_1} dt_2 k^2(t_2)\int_0^{t_2} dt_3 e^{-t_3}k^{-2}(t_3)$$

$$\left. \times \left(\frac{1}{t_3}-\frac{1-e^{-t_3}}{t_3^2}\right)\right] \simeq 0.038. \quad (B5)$$

At the same density ρ_{JL}, the equilibrium value is $L(\langle\rho^2\rangle-\langle\rho\rangle^2)_{eq} = 0.0476$.

[1] S. Edwards and R. Oakeshott, Physica A **157**, 1080 (1989).
[2] A. Mehta and S. Edwards, Physica A **157**, 1091 (1989).
[3] S. Edwards, in *Granular Matter: An Interdisciplinary Approach*, edited by A. Mehta (Springer-Verlag, New York, 1994).
[4] S. Edwards and D. Grinev, Phys. Rev. E **58**, 4758 (1999).
[5] J.B. Knight, C.G. Fandrich, C.N. Lau, H.M. Jaeger, and S.R. Nagel, Phys. Rev. E **51**, 3957 (1995).
[6] E.R. Nowak, J.B. Knight, E. Ben-Naim, H.M. Jaeger, and S.R. Nagel, Phys. Rev. E **57**, 1971 (1998).
[7] E. Ben-Naim, J.B. Knight, E.R. Nowak, H.M. Jaeger, and S.R. Nagel, Physica D **123**, 380 (1998).
[8] C. Josserand, A. Tkachenko, D. Mueth, and H. Jaeger, Phys. Rev. D **85**, 3632 (2000).
[9] P. Philippe and D. Bideau, Europhys. Lett. **60**, 677 (2002).
[10] L. Cugliandolo, J. Kurchan, and L. Peliti, Phys. Rev. E **55**, 3898 (1997).
[11] A. Crisanti and F. Ritort, J. Phys. A **36**, R181 (2003).
[12] H.A. Makse and J. Kurchan, Nature (London) **415**, 614 (2002).
[13] A. Liu and S. Nagel, *Jamming and Rheology: Constrained Dynamics* (Taylor and Francis, London, 2001).
[14] J. Kurchan, J. Phys.: Condens. Matter **12**, 6611 (2000).
[15] A. Barrat, J. Kurchan, V. Loreto, and M. Sellito, Phys. Rev. Lett. **85**, 503 (2000).
[16] A. Barrat, J. Kurchan, V. Loreto, and M. Sellito, Phys. Rev. E **63**, 051301 (2001).
[17] D. Dean and A. Lefèvre, Phys. Rev. Lett. **86**, 5639 (2001).
[18] A. Lefèvre and D. Dean, Phys. Rev. E **64**, 046110 (2001).
[19] A. Lefèvre and D. Dean, J. Phys. A **34**, L213 (2001).
[20] D. Dean and A. Lefèvre, e-print cond-mat/0212297.
[21] A. Lefèvre, J. Phys. A **35**, 9037 (2002).
[22] M. Sellitto, Phys. Rev. E **66**, 042101 (2002).
[23] A. Coniglio, A. Fierro, and M. Nicodemi, Physica A **302**, 193 (2001).
[24] A. Fierro, M. Nicodemi, and A. Coniglio, Europhys. Lett. **59**, 642 (2002).
[25] A. Fierro, M. Nicodemi, and A. Coniglio, Phys. Rev. E **66**, 061301 (2002).
[26] M. Nicodemi, A. Fierro, and A. Coniglio, Europhys. Lett. **60**, 684 (2002).
[27] A. Prados, J. Brey, and B. Sánchez-Rey, Physica A **284**, 277 (2000).
[28] A. Prados and J. Brey, Phys. Rev. E **66**, 041308 (2002).
[29] J. Brey and A. Prados, J. Phys.: Condens. Matter **14**, 1489 (2002).
[30] A. Prados and J. Brey, e-print cond-mat/03044654.
[31] G.D. Smedt, C. Godrèche, and J. Luck, Eur. Phys. J. B **27**, 363 (2002).
[32] G.D. Smedt, C. Godrèche, and J. Luck, Eur. Phys. J. B **32**, 215 (2003).
[33] J. Berg, S. Franz, and M. Sellitto, Eur. Phys. J. B **26**, 349 (2002).
[34] X. Jin, G. Tarjus, and J. Talbot, J. Phys. A **27**, L195 (1994).
[35] P.L. Krapivsky and E. Ben-Naim, J. Chem. Phys. **100**, 6778 (1994).

[36] G. Tarjus, P. Schaaf, and J. Talbot, J. Chem. Phys. **93**, 8352 (1990).

[37] J. Talbot, G. Tarjus, and P. Viot, Phys. Rev. E **61**, 5429 (2000).

[38] J. Talbot, G. Tarjus, and P. Viot, J. Phys. A **32**, 2997 (1999).

[39] J. Talbot, G. Tarjus, and P. Viot, Eur. Phys. J. E **5**, 445 (2001).

[40] J. Talbot, G. Tarjus, and P. Viot, Fractals **11**, 185 (2003).

[41] A. Kolan, E. Nowak, and A. Tkachenko, Phys. Rev. E **59**, 3094 (1999).

[42] J. Evans, Rev. Mod. Phys. **65**, 1281 (1993).

[43] J. Talbot, G. Tarjus, P.V. Tassel, and P. Viot, Colloids Surf., A **165**, 287 (2000).

[44] A. Rényi, Sel.Trans.Math.Stat.Prob. **4**, 205 (1963).

[45] B. Bonnier, D. Boyer, and P. Viot, J. Phys. A **27**, 3671 (1994).

[46] P. Viot, G. Tarjus, and J. Talbot, Phys. Rev. E **48**, 480 (1993).

[47] A. Rosato, K. Strandburg, F. Prinz, and R. Swendsen, Phys. Rev. Lett. **58**, 1038 (1987).

[48] M. Möbius, B. Lauerdale, S. Nagel, and H. Jaeger, Nature (London) **414**, 270 (2001).

[49] D. Hong, P. Quinn, and S. Luding, Phys. Rev. Lett. **86**, 3423 (2001).

[50] A.P.J. Breu, H.-M. Ensner, C.A. Kruelle, and I. Rehberg, Phys. Rev. Lett. **90**, 014302 (2002).

[51] If one interprets the line as a layer of grains in a vibrated column, $(1/z)$ is not quite the ''bulk'' compactivity that would describe the whole system. Indeed the relevant 3D volume à la Edwards (for fixed total number of particles in the whole column) corresponds here to L^2/N for L fixed. The bulk compactivity would then be $X = (1/L^2)[\partial S/\partial(1/N)]_L$, which gives $X^{-1} = \rho^2(z + \ln[z/1 - e^{-z}])$.

[52] I.Z. Fisher, *Statistical Theory of Liquids* (University of Chicago Press, Chicago, 1964).

[53] B. Widom, J. Chem. Phys. **44**, 3888 (1966).

[54] G. Tarjus, P. Schaaf, and J. Talbot, J. Stat. Phys. **63**, 167 (1991).